Journal of Imaging Science and Technology® 50(2): 125–138, 2006.

Optimized *RGB* for Image Data Encoding

Beat Münch and Úlfar Steingrímsson
Swiss Federal Laboratories for Material Testing and Research (EMPA), Dübendorf, Switzerland
E-mail: beat.munch@empa.ch

Abstract. *The present paper discusses the subject of an RGB optimization for color data coding. The current RGB situation is analyzed and those requirements selected which exclusively address the data encoding, while disregarding any application or workflow related objectives. In this context, the limitation to the RGB triangle of color saturation, and the discretization due to the restricted resolution of 8 bits per channel are identified as the essential drawbacks of most of today's RGB data definitions. Specific validation metrics are proposed for assessing the codable color volume while at the same time considering the discretization loss due to the limited bit resolution. Based on those measures it becomes evident that the idea of the recently promoted e-sRGB definition holds the potential of being qualified as a global RGB data standard without imposing restrictions in regard to feasible surface colors. Optimizing strategies are thus suggested and adapted to the e-sRGB concept focusing on 8 bits per channel. The resulting RGB makes it possible to store a color value to a 32 bit word, yet covering the entire gamut of all existing surface colors at a resolution above the perceptible limit for any color sector, thus satisfying the requirements of a universal RGB which is particularly optimized for color image data encoding. © 2006 Society for Imaging Science and Technology.*
[DOI: 10.2352/J.ImagingSci.Technol.(2006)50:2(125)]

INTRODUCTION

RGB is undoubtedly the most popular color encoding form; its wide acceptance is due to the fact that it is similar to humans' color perception, and to the technique used with picture tubes, where color reproduction is achieved by aiming three separate electron beams onto red, green, and blue phosphorus targets. The search for the best suited *RGB* specifications involves many aspects and has been a research topic for many years now. Various *RGB* specifications have been promoted in the past, and some of them are in common use. Because different *RGB* encodings have varying suitability for different uses, none of them has become accepted as a distinct universal standard yet. No *RGB* will probably ever be able to meet arbitrary colorimetric requirements for any given application. Hence, the usage of *RGB* is somewhat nonuniform.

Nevertheless, *RGB* is often regarded as a colorimetric *de facto* standard and thus, many important color image data formats (JPEG, TIFF) refer to *RGB* without providing its precise specifications. However, since *RGB* primaries, white point as well as the gamma exponent making up the accurate definition of an *RGB* might disagree considerably, serious color shifts will occur if incorrect assumptions are made.

Received Dec. 23, 2004; accepted for publication Apr. 21, 2005.
1062-3701/2006/50(2)/125/14/$20.00.

Indeed, image data originating from digital cameras and scanners are highly device dependent, and the same variability exists for image reproducing devices such as monitors and printers. Figure 1 shows the locations of the primaries for a few important *RGB* color spaces, revealing a manifold variety. The respective specifications for the primaries, white points and gamma values are given in Table I.

In practice, the problem of *RGB* misinterpretation has been approached by either providing an ICC profile or by assuming *sRGB* if no ICC profile is present. For some time this practice was adhered to, with digital cameras producing exclusively *sRGB*, and Photoshop offering the option of embedding ICC profiles whenever other *RGB* color encodings are saved. However, inter-operability is still a problem because ICC profiles are not always embedded, and more importantly are not understood by many readers. Furthermore, in some cases, other metadata fields are used to indicate *RGB* image data other than *sRGB*. The Exif format, for instance—actually providing a JPEG format extended with metadata—is already being widely used by many of the latest

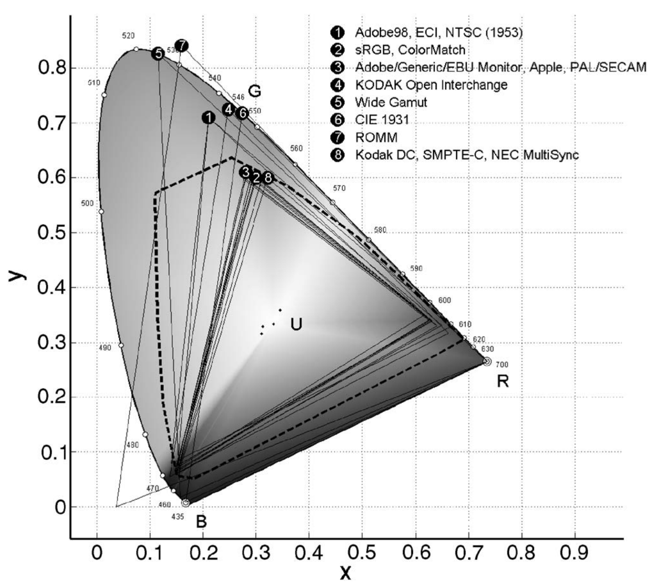

Figure 1. Overview of common *RGB* spaces Refs. 2, 3, 6, 14, 16, and 32 adopted by digital cameras, scanners, monitors, or merely serving as working color spaces for image analysis and archiving purposes. Table I contains the corresponding specifications. The figure shows the xy color space representation with the horseshoe shaped spectral color shape, which also denotes the optimal surface color boundaries. The dashed polyeder marks the convex hull around the real-world surface colors.

Table I. A list of some well-known and often used *RGB* color spaces (Refs. 2, 3, 6, 11, 14, 16, and 32). The corresponding specifications are given in Table I.

Adobe 1998	Generic Monitor	SMPTE
Adobe Monitor	Kodak DC	*sRGB*
Apple	Kodak Open Interchange	Wide Gamut
Bruce Fraser	NEC Multi Sync Monitor	XYZ
Color Match	NTSC 1953	*e-sRGB* 8/9/10 bits
ECI	PAL	
Generic EBU Monitor	ROMM	

digital cameras and provides accurate *RGB* specifications. Such metadata fields can, however, conflict with embedded ICC profiles, and also may not be widely supported by readers.

The most favorable approach to the *RGB* misinterpretation problem would certainly be a universal *RGB* data standard satisfying the most important basic requirements. As stated above, this request is not realistic because of the need for different image states and reference media. However, since the *RGB* concept itself is based on the trichromatic theory of color vision and the underlying CIE standard observer tristimulus values of spectral colors,[1] chromaticity values built on any *RGB* type may be easily converted into any other *RGB* system at moderate expense, provided that the specifications of the original *RGB* types are known. Consequently, a hypothetical *RGB* exclusively designed to form a data link between miscellaneous input and output *RGB* devices must not necessarily accomplish application or workflow specific needs.

The only remaining requirement on this hypothetical *RGB* is the ability to encode any arbitrary or at least most of all existing real-world colors with a satisfactory resolution. Yet, all of the currently well-known *RGB* standard color spaces suffer from considerable restrictions either in respect of the codable color range, of the resolution due to discretization, or of both. The principal background of these drawbacks is the limitation of current *RGB* encodings to 8 bits per channel.

Nevertheless, various 8 bit standardization attempts have been promoted more or less successfully. At present it can be observed that mainly *sRGB*[2–4] which is designed according to the response of a reference CRT display, as well as ADOBE98 *RGB* are predominant in graphic arts, printing and the digital camera industry. Data of the *sRGB* type can easily be interpreted by any common CRT monitor without applying additional color transformation. However, while *sRGB* meets the needs of Internet color imaging well, the achievable saturation bandwidth is rather narrow compared to the color range of many non-CRT applications such as digital photofinishing, or of the potential of CCD arrays of modern digital cameras and scanners. Although *sRGB* clearly exceeds the real-world surface colors in certain color sectors, it can easily be verified in three-dimensional (3D) Lab that for instance in the blue area, parts of even the ISO standard newsprint color space[5] (std. illum. D50) are located just at the border or even outside the boundaries of *sRGB* (std. illum. D65), depending on the color appearance model used to adapt D50 to D65.

Digital camera manufacturers often provide raw *RGB* images that are very device specific and thus lack general applicability. Nevertheless due to the popularity of *sRGB*, many camera manufacturers additionally support *sRGB*. However, this involves transferring the colors recorded from the CCD array into the boundaries of the *sRGB* space by applying a convenient color rendering. This procedure inevitably yields a certain nonlinear, noncontinuous, and nonuniform gamut mapping, and thus comprises irreversible color changes, although good color rendering algorithms minimize the loss of scene color information. Since the receiver of an *sRGB* image rarely knows what color rendering was applied, he is hardly able to undo it in order to get back to the scene colorimetry and to make optimal use of the comparatively large CCD chromaticities.

Concerning monitors and printers, the color spaces of such output devices are not equivalent to *sRGB* either and thus the color data has to be mapped for colorimetrically correct image reproduction as well.

RGB definitions are classified in various ways. Susstrunk[6] splits up *RGB* spaces into categories. Device specific *RGB* types are divided into sensor *RGB* and output *RGB*. Intermediary and device neutral *RGB* color spaces for image processing and archiving purposes such as *ISO RGB* and CIE *XYZ* (actually a virtual *RGB*) are considered as unrendered spaces suitable for the definition of colorimetric estimates of image scenes, while rendered spaces such as *sRGB* and ADOBE98 *RGB* represent colorimetric estimates for color reproduction. Common standard *RGB* color spaces for storing image data often belong to this *RGB* category and represent virtual output devices.

Colorimetric limitations of *RGB* may be partially overcome by performing the right processing tricks,[7] but they usually end up narrowing the achievable color gamut. Regarding to the most significant limitation of *RGB* spaces coming from their truncation of high saturation values, miscellaneous solutions have been proposed, as for instance the assignment of CIE Luv instead of *RGB*, or making use of oversized *RGB*'s such as ROMM- or RIMM-*RGB*,[8,9] or storing color values outside the *RGB* triangle in a separate data layer.[10] Recent standardization attempts making it possible to go beyond the RGB boundaries are the *extended* s*RGB* *e-sRGB* from Hewlett Packard[11,12] and *scRGB* from Microsoft, which offer a sufficiently large color space and thus inhibit color restrictions. As a consequence, however, these standards require a data range of more than 8 bits per *RGB* channel. Whereas *e-sRGB* provides 10, 12, or 16 bits, *scRGB* always works with 16 bits, and thus needs twice as much data space as conventional formats. Of course it is desirable to come up with a single 32 bit data word that would include all *R*, *G*, and *B* channels.

This article addresses the topic of an optimal *RGB* definition in terms of economic data encoding. A "good" *RGB*, on the one hand, needs to include as many of all the existing real-world colors as possible, and on the other hand, it is expected to provide a sufficient resolution for all hues. If the colors of a scene are neither produced by self illuminants nor lightened by optical brighteners but solely by conventional surface reflection, a good *RGB* definition should at least contain most of the real-world surface colors (see Sec. 3.1). This requirement calls for a suitable estimation metrics and justifies the corresponding evaluation of various kinds of *RGB* spaces.

Yet for real-world applications and workflows, *RGB* suitability might be validated in lots of different ways. In Ref. 13, a few essential requirements for defining color spaces are discussed and divided into colorimetric, color appearance, and device-dependent needs. Finlayson[14] particularly tweaks for hue constancy. This was also one of the criteria for the development of an oversized ROMM *RGB*.[8] Granger[15] on the other hand optimizes *RGB* for uniformity. Kang[16] reports the computational accuracy of various *RGB* encoding standards by measuring a printed set of color patches. Katajamäki[17] estimates the optimal gamma value for a specific *RGB* image in terms of a most even distribution of the image colors. Hill[18] exposes the fundamentals for comparative color space analysis based on examinations in visually equispaced color systems such as CIE Lab. Against this background, Braun and Spaulding[19] propose volume based metrics for rating color encoding, considering to what degree an encoding encloses the "real-world surface colors." Separately, they evaluate the quantization related color space limits by determining the maximum and the average quantization errors depending on the bit resolution.

The latter papers include metrics qualified for assessing various types of color spaces such as *YCC*, *CIE Lab*, *RGB*, and *e-sRGB*. Although the same holds true for the parameters about to be proposed here below, the specific goal of this paper is to rank color spaces of the *RGB* type only, in order to account for the promotion of a general *RGB* for color data encoding.

CURRENT *RGB* PRACTICE

Current *RGB* systems are ultimately based on the CIE *XYZ* standard observer space.[1] *RGB* spaces are basically derived from CIE *XYZ* by simple matrix transformation. On the one hand, due to the exponential progression of luminance as a function of cathode voltage for wide-spread CRT monitor techniques, and on the other hand, due to the validity of Weber's law[20] for the sensitivity of the eye, RGB values also undergo a power function with the so-called gamma exponent γ which is a handy approximation of the exponential function. The motivation of the gamma value is outlined in.[12] In general, such converted *RGB* chroma values are subsequently mapped to the encoding space of usually $n=8$ bits per channel by simply scaling by a factor (2^n-1). Thus, only RGB chromaticity values in the range of $[0,\ldots 1]$ become codable while values below zero or larger than one are skipped, yielding a triangular shaped *RGB* limitation.[1] Most of all *RGB* definitions currently in use are defined according to this encoding scheme.

The primary objections against conventional *RGB* in terms of data encoding are, firstly, the restricted color gamut, and secondly, the limited color resolution close to the visual perception limit. In conventional *RGB* coding, the color gamut is confined by the triangular shape spanned by the *RGB* primaries. Accordingly, the first objective is exclusively associated with the encoding boundaries of [0,1] with respect to the x,y color table values of each *RGB* channel. The second one depends on the quantization limits associated with the applied bit rate of usually $n=8$.

A remedy for both objections is provided by *e-sRGB* proposed by Hewlett Packard.[11] Basically, *e-sRGB* has the same definition of the white point, the primary colors and the gamma value as the well established *e-sRGB* standard. Its supplementary benefits are firstly, the expanded encoding boundary, and secondly, the enhanced bit resolution. By applying a linear mapping of the available data encoding range, the disposable color interval of each *RGB* channel is expanded to $[-0.53, 1.68]$ making possible a color range which is sufficiently wide for covering all virtually feasible surface colors according to Schrödinger.[21] Notice that by this approach the codable color range is expanded to a scope far beyond the optimal surface colors. In addition, a resolution of 10, 12, or 16 bits per *RGB* channel is provided, selectively.

The forward *e-sRGB* encoding is specified below.

At first, the conversion from tristimulus values to linear *e-sRGB* values

$$\begin{bmatrix} R_{e\text{-}sRGB} \\ G_{e\text{-}sRGB} \\ B_{e\text{-}sRGB} \end{bmatrix} = \begin{bmatrix} 3.2406 & -1.5372 & -0.4986 \\ -0.9689 & 1.8758 & 0.0415 \\ 0.0557 & -0.2040 & 1.0570 \end{bmatrix} \cdot \begin{bmatrix} X_N \\ Y_N \\ Z_N \end{bmatrix}. \tag{1}$$

For each color channel $C_{e\text{-}sRGB} \in \{R_{e\text{-}sRGB}, G_{e\text{-}sRGB}, B_{e\text{-}sRGB}\}$:

$$C'_{e\text{-}sRGB} = \begin{cases} \beta \cdot C_{e\text{-}sRGB}{}^{1/\gamma} - \alpha, & \forall C_{e\text{-}sRGB} > \tau \\ -(\beta \cdot (-C_{e\text{-}sRGB})^{1/\gamma} - \alpha), & \forall C_{e\text{-}sRGB} < -\tau \\ 12.92 \cdot C_{e\text{-}sRGB}, & \forall -\tau \leqslant C_{e\text{-}sRGB} \leqslant \tau \end{cases}, \tag{2}$$

with

$$\alpha = 0.055, \quad \beta = 1.055, \quad \gamma = 2.4, \quad \tau = 0.003\,1308. \tag{3}$$

Finally, the linear mapping into the encoding range for each color channel $C'_{e\text{-}sRGB} \in \{R'_{e\text{-}sRGB}, G'_{e\text{-}sRGB}, B'_{e\text{-}sRGB}\}$ is given by:

$$C''_{e\text{-}sRGB} = C'_{e\text{-}sRGB} \cdot \varepsilon + \omega \tag{4}$$

with

$$\varepsilon = 255 \cdot 2^{n-9}$$

$$\omega = 2^{n-2} + 2^{n-3}$$

where $n \in \{10,12,16\}$ is the number of bits used for each R,G,B channel.

The appropriate inverse *e-sRGB* encoding is reported subsequently.

For each color channel $C''_{e\text{-}sRGB} \in \{R''_{e\text{-}sRGB}, G''_{e\text{-}sRGB}, B''_{e\text{-}sRGB}\}$:

$$C'_{e\text{-}sRGB} = \frac{C''_{e\text{-}sRGB} - \omega}{\varepsilon} \tag{5}$$

with

$$\varepsilon = 255 \cdot 2^{n-9}$$

$$\omega = 2^{n-2} + 2^{n-3}$$

where $n \in \{10,12,16\}$ is the number of bits used for each R,G,B channel.

$$C_{e\text{-}sRGB} = \begin{cases} [(\alpha + C'_{e\text{-}sRGB}) \div \beta]^{\gamma}, & \forall C'_{e\text{-}sRGB} > \tau' \\ -\ [(\alpha - C'_{e\text{-}sRGB}) \div \beta]^{\gamma}, & \forall C'_{e\text{-}sRGB} < -\tau' \\ C'_{e\text{-}sRGB} \div 12.92, & \forall -\tau' \leqslant C'_{e\text{-}sRGB} \leqslant \tau' \end{cases}, \tag{6}$$

with

$$\alpha = 0.055, \quad \beta = 1.055, \quad \gamma = 2.4, \quad \tau' = 0.040\,45. \tag{7}$$

Finally with $C_{e\text{-}sRGB} \in \{R_{e\text{-}sRGB}, G_{e\text{-}sRGB}, B_{e\text{-}sRGB}\}$, the conversion from linear *e-sRGB* values to tristimulus values normalized to the reference display black and white:

$$\begin{bmatrix} X_N \\ Y_N \\ Z_N \end{bmatrix} = \begin{bmatrix} 0.4124 & 0.3576 & 0.1805 \\ 0.2126 & 0.7152 & 0.0722 \\ 0.0193 & 0.1192 & 0.9505 \end{bmatrix} \cdot \begin{bmatrix} R_{e\text{-}sRGB} \\ G_{e\text{-}sRGB} \\ B_{e\text{-}sRGB} \end{bmatrix}. \tag{8}$$

The functional form of the *e-sRGB* nonlinearity is given by the connection between C_{e-sRGB} and C'_{e-sRGB}, which is essentially determined by a power function with exponent γ. To prevent having an infinite slope near zero, a linear term was substituted for the power function at small values below τ. In order to achieve a continuous junction of this straight line and the power function, a transition point at $\tau = 0.003\,130\,8$ (and $\tau' = 0.040\,45$ for the backward transform) was defined. This scheme originates from the definition of the *sRGB* standard. It is indicated to rectify in this context that accurately complying with the continuity conditions merely yields

$$\tau = \left(\frac{\alpha \cdot \gamma}{\beta \cdot (\gamma - 1)}\right)^{\gamma} = 0.003\,039\,934 \tag{9}$$

and

$$\tau' = \frac{\alpha \cdot \gamma}{\gamma - 1} - \alpha = 0.039\,285\,714, \tag{10}$$

which differs slightly from the standard definitions in Eqs. (3) and (7). However, in *sRGB*, the difference is irrelevant, since the 8 bit discretization is coarse enough. For *e-sRGB* providing a resolution of up to 16 bits per channel, the discrepance results in a nonessential but unesthetic discontinuity.

METRICS FOR ESTIMATING *RGB* DATA ENCODING SKILL

The central attribute for the assessment of *RGB* encoding is the ratio of arbitrarily existing colors covered by a specific encoding. As stated in Sec. 1, this value is constricted for most of the *RGB* types currently in existence due to the *RGB* triangle boundaries as well as due to the limited bit resolution.

In principle, the gamut of existing colors is not restricted with regard to any colorimetric limits, since self-illuminants can achieve arbitrary lightness and saturation values. In contrast, the potential color space arising from illuminated surfaces is bounded depending on the illuminant characteristics. A distinction is drawn between theoretically possible and practically attainable surface colors, i.e., the optimal surface colors and the real-world surface colors. The gamuts over which those two surface color types run is briefly discussed in the next section. For the current work, the question as to whether a color value is contained within the optimal and/or real-world surface color gamut is generally examined in 3D.

Optimal and Real-World Surface Colors

In real life images, the main fraction of all colors is endowed with surface colors, resulting from objects illuminated by a certain lighting. Since a passive object cannot reflect more than the light it is illuminated by, the gamut of all surface colors is delimited. According to the theoretical work of Schrödinger,[21] the hull around all virtually existing nonfluorescent surface colors is confined by the *optimal surface colors* defined by all spectral reflections featuring either one single continuous transmission band, or one single continuous absorption band, alternatively. In the color table representation, the optimal surface color boundary is characterized by the horseshoe shaped CIE spectrum locus[1] which is visualized in Fig. 1.

In real world, only approximately half of all colors within the optimal surface color gamut are effectively feasible.[22,23] For the determination of *real-world surface colors*, a large set of real-world surface color samples was collected and its convex hull defined in *XYZ* (see Sec. 3.4), assuming that additive color compositions are practicable. The real-world surface colors include Pointer,[22] Pantone, Munsell, and SOCS[24] colors converted to the specifically required illuminants by using Bradford color adaptation.[25] In Fig. 1, the two-dimensional (2D) convex hull around the real-world surface colors is illustrated by a dashed polyeder.

Estimation Criteria

A *RGB* color space explicitly optimized with respect to image data encoding should satisfy three main criteria:

(1) It should be large enough for encoding all real-world surface colors (see Sec. 3.1).
(2) Colors outside the optimal surface color gamut cannot be implemented except by self illuminants or by fluorescent materials. They also cannot be reproduced by any printing devices. Thus, coding of colors outside the range of real-world surface colors should be given a priority lower than given those inside it.
(3) The visual color distances between two adjacent color codes—being limited due to employing usually 8 bits per *RGB* channel—should be smaller than the visually perceivable minimal color distance, that is, less than 1 ΔE_{76}[26] for all color domains.

Previous estimation metrics[18,19] take consideration of the main criteria (1)–(3) in a separated manner. The focus of this section is to propose one single metric incorporating all of them.

The following requirements are of additional but minor importance for exclusive data encoding:

(4) A position of the *RGB* primaries close to the primaries of real image reproducing devices (monitors, printers).
(5) A color neutral gray axis.

Criterion (4) addresses the facility of quick and easy image display and is thus for convenience only. It should be completely disregarded because the range of existing device specific *RGB* definitions is too wide.

Criterion (5) is implicitly fulfilled whenever the *RGB* specifications are given by its 2D *xy* color table values (with 6 degrees of freedom) together with the colorimetric white point reference (with 3 degrees of freedom), instead of assessing the 9 degrees of freedom by the primaries in 3D *XYZ* specifications. The location of the white point is thereby exclusively responsible for the colors in the gray axis.

To prove this, let a color value $\mathbf{R}=(R,G,B)$ be a gray color with $\mathbf{R}_{(R=G=B=U)}=\mathbf{U}$. Solving the equation system

$$\mathbf{xyY}(\mathbf{XYZ}(\mathbf{U})) = \mathbf{xyY}_W, \tag{11}$$

$$\mathbf{xy}(\mathbf{XYZ}(R,0,0)) = \mathbf{xy}_R, \tag{12}$$

$$\mathbf{xy}(\mathbf{XYZ}(0,G,0)) = \mathbf{xy}_G, \tag{13}$$

$$\mathbf{xy}(\mathbf{XYZ}(0,0,B)) = \mathbf{xy}_B, \tag{14}$$

with the color conversions $\mathbf{xyY}[\mathbf{XYZ}(\mathbf{RGB})]$ from *RGB* coordinates over CIE *XYZ* using a matrix transform, and from *XYZ* to *xyY* color tables as described in Ref. 1, and after including the white point $\mathbf{xyY}_W=(x_W,y_W,100)$ and the primary color table values $\mathbf{xy}_R=(x_R,y_R)$, $\mathbf{xy}_G=(x_G,y_G)$ and $\mathbf{xy}_B=(x_B,y_B)$, then the CIE *XYZ* chromaticities of the gray colors become

$$X(\mathbf{U}) = \frac{U \cdot x_W}{y_W}, \tag{15}$$

$$Y(\mathbf{U}) = U, \tag{16}$$

$$Z(\mathbf{U}) = \frac{U \cdot (1 - x_W - y_W)}{y_W}, \tag{17}$$

and thus are independent of the primaries *xy* values. Hence, the color neutrality of the gray axis is exclusively determined by the white point.

Estimation of the Main Criteria for a Data RGB

The basic idea for a model for the evaluation of the three main objectives [criteria (1)–(3)] includes two issues:

(1) The color volume as well as the discretization considerations are accomplished in CIE *Lab*, which as a good approximation can be assumed to be perceptibly uniform.
(2) Each data sample encodes the color scope of a parallelepiped with a side lengths of $\Delta E_{76}=1$ at most, assuming that the eye is capable of perceiving color differences of $\Delta E_{76}>1$. This means that if adjacent color codes are less than $\Delta E_{76}=1$ apart from each other, the spanned color volume corresponds to the volume of the parallelepiped. If one or more color distances are larger than 1, they are truncated. Thus, each particular color code may cover the volume of a parallelepiped with maximal side lengths of unit ΔE_{76}.

The spacings between two adjacent color codes

$$\mathbf{\Delta_{RGB}} = \begin{pmatrix} R \\ G \\ B \end{pmatrix} - \begin{pmatrix} R+\Delta_r \\ G+\Delta_g \\ B+\Delta_b \end{pmatrix} = \mathbf{RGB} - \mathbf{RGB}_{\Delta_{r,g,b}},$$

$$\Delta_{r,g,b} \in [0,1], \tag{18}$$

are converted to CIE *Lab* resulting in three vectors limited to $1\Delta E_{76}$ each, spanning a single color fragment, yielding

$$\boldsymbol{\Delta Lab}_r = |\boldsymbol{Lab}_{(\mathbf{RGB})} - \boldsymbol{Lab}_{(\mathbf{RGB}+\boldsymbol{\Delta}_r)}|, \quad \boldsymbol{\Delta}_r = (1,0,0), \tag{19}$$

$$\boldsymbol{\Delta Lab}_g = |\boldsymbol{Lab}_{(\mathbf{RGB})} - \boldsymbol{Lab}_{(\mathbf{RGB}+\boldsymbol{\Delta}_g)}|, \quad \boldsymbol{\Delta}_g = (0,1,0), \tag{20}$$

$$\boldsymbol{\Delta Lab}_b = |\boldsymbol{Lab}_{(\mathbf{RGB})} - \boldsymbol{Lab}_{(\mathbf{RGB}+\boldsymbol{\Delta}_b)}|, \quad \boldsymbol{\Delta}_b = (0,0,1). \tag{21}$$

Table II. White points, gamma values, and primary colors of the standard *RGB* encodings considered.

	White	γ	*Rx*	*Ry*	*Gx*	*Gy*	*Bx*	*By*
Adobe98	D65	2.20	0.6400	0.3300	0.2100	0.7100	0.1500	0.0600
Adobe Monitor	D65	1.81	0.6300	0.3400	0.2950	0.6050	0.1550	0.0770
Apple	D65	1.80	0.6250	0.3400	0.2800	0.5950	0.1550	0.0700
CIE 1931, E, 2.2	E	2.20	0.7350	0.2650	0.2740	0.7170	0.1670	0.0090
ColorMatch	D50	1.80	0.6300	0.3400	0.2950	0.6050	0.1550	0.0770
ECI	D50	1.80	0.6700	0.3300	0.2100	0.7100	0.1400	0.0800
Generic EBU Monitor (γ=1.8)	D50	1.60	0.6314	0.3391	0.2809	0.5971	0.1487	0.0645
Generic Monitor	D50	1.90	0.6277	0.3427	0.2803	0.6097	0.1491	0.0636
Kodak DC	D50	2.22	0.6492	0.3314	0.3219	0.5997	0.1548	0.0646
KODAK Open Interchange	D50	1.72	0.6619	0.3173	0.2473	0.7243	0.1378	0.0554
NEC MultiSync Monitor (γ=1.8)	D50	1.60	0.6167	0.3503	0.2957	0.5884	0.1481	0.0697
NTSC (*1953*)	C	2.20	0.6700	0.3300	0.2100	0.7100	0.1400	0.0800
PAL/SECAM	D65	2.20	0.6400	0.3300	0.2900	0.6000	0.1500	0.0600
ROMM	D50	1.80	0.7347	0.2653	0.1596	0.8404	0.0366	0.0001
SMPTE-C	D65	2.20	0.6300	0.3400	0.3100	0.5950	0.1550	0.0700
sRGB IEC61966-2.1	D65	2.20	0.6400	0.3300	0.3000	0.6000	0.1500	0.0600
Wide Gamut	D50	2.20	0.7347	0.2653	0.1152	0.8264	0.1566	0.0177

The new volumetric color gamut estimate arises from the sum of all volume fractions, which are constrained to the smallest perceptible δ, e.g., 1 ΔE_{76}:

$$\boldsymbol{\Delta Lab}''_r = \min(\boldsymbol{\Delta Lab}_r, \delta) \tag{22}$$

$$\boldsymbol{\Delta Lab}''_g = \min(\boldsymbol{\Delta Lab}_g, \delta) \tag{23}$$

$$\boldsymbol{\Delta Lab}''_b = \min(\boldsymbol{\Delta Lab}_b, \delta) \tag{24}$$

For δ, alternative color distance metrics different from ΔE_{76} have not been considered, because more recent distance metrics like ΔE_{94} and ΔE_{2000}, or color appearance models such as CIECAM97 or CIECAM02 do not provide a corresponding 3D color space system as *Lab* does in the case of ΔE_{76}. This is, however, required to examine color spaces in its 3D geometrical context, as is accomplished with the metrics below.

The sum of all color fragments being encodable with n bits and additionally being located within the range of the real-world surface colors $\mathcal{V}_{\mathrm{ref}}$ yields the *effectively codable color volume* of a specific RGB space, a new metric for the assessment of RGB spaces with respect to the coding suitability:

$$V_{Lab} = \sum_{\boldsymbol{Lab}_{(\mathbf{RGB})} \in \mathcal{V}_{\mathrm{ref}}} \det[\boldsymbol{\Delta Lab}''_r, \boldsymbol{\Delta Lab}''_g, \boldsymbol{\Delta Lab}''_b]. \tag{25}$$

In the following, this measure is generally given relative to the volume of the real-world surface color gamut

$$V_{\mathrm{ref}} = \int_{\mathcal{V}_{\mathrm{ref}}} dv, \tag{26}$$

yielding

$$v_{Lab} = \frac{V_{Lab}}{V_{\mathrm{ref}}}. \tag{27}$$

Further commonly used metrics are the conventional mean, mean square and maximal color distance between two adjacent codes in a color space

$$\vartheta_{Lab} = \frac{1}{3 \cdot n} \sum_{\boldsymbol{Lab}_{(\mathbf{RGB})} \in V_{\mathrm{ref}}} |\boldsymbol{\Delta Lab}_r| + |\boldsymbol{\Delta Lab}_g| + |\boldsymbol{\Delta Lab}_b|, \tag{28}$$

$$\vartheta''_{Lab} = \frac{1}{3 \cdot n} \sqrt{\sum_{\boldsymbol{Lab}_{(\mathbf{RGB})} \in V_{\mathrm{ref}}} |\boldsymbol{\Delta Lab}_r|^2 + |\boldsymbol{\Delta Lab}_g|^2 + |\boldsymbol{\Delta Lab}_b|^2}, \tag{29}$$

$$\psi_{Lab} = \max[\boldsymbol{\Delta Lab}_r, \boldsymbol{\Delta Lab}_g, \boldsymbol{\Delta Lab}_b]_{\forall \boldsymbol{Lab}_{(\mathbf{RGB})} \in V_{\mathrm{ref}}}. \tag{30}$$

Verification

According to Sec. 3.3, determining the codable color volume by summing up the volume fragments provides the advantage of being able to truncate the side lengths of each single encoding fraction to a well defined maximum size, which corresponds with the visual capabilities.

Without providing this benefit, the color volume could be calculated much more efficiently by using convex hull techniques.[27,28] Since any color space in the CIE *Lab* system may easily contain concave surfaces—parts of the planes delimiting *RGB* gamuts behave likewise—a gimmick is required whenever convex hull techniques are used. According to Grassmann's law the CIE *XYZ* color space obeys the rules of linearity and additivity. Hence, a color space in *XYZ* is supposed to be convex, provided that additive color mixtures are allowed. The transformation of a convex surface from CIE *XYZ* into CIE *Lab* then brings back the concavities, provided that the surface is sufficiently well sampled.[29]

Based on comparisons with the results of the above convex hull technique, the accuracy of the color volume determination by summing up discrete parallelepipeds according to Eqs. (19)–(25)—while omitting the constraints to 1 ΔE_{76}—was examined. The average of the two unequal calculations disagrees by $\leqslant 1\%$ only, making it evident that the summing up approach yields results of satisfactory accuracy.

Evaluation of Some Well-Known** RGB **Types

A few well-known *RGB* color spaces[14,16,6] as listed in Table II have been judged according to the metrics of Sec. 3.3.

XYZ is included in this list, since it can be interpreted as a virtual *RGB* and shows interesting results. The *e-sRGB* type[11] must be considered as a special *RGB* case, since *e-sRGB* by default assigns 10, 12, or 16 bits per channel instead of 8 bits only. Thus, a direct comparison of *e-sRGB* with other *RGB* types would be unfair. Consequently, the *e-sRGB* standard was evaluated for 8 bits per channel, as well as for 9 and 10 bits for pointing out the associated improvement. In fact, however, the current *e-sRGB* standard provides neither a resolution of 8 bits nor of 9 bits.

The color volumes encodable by these *RGB* types have been evaluated by extracting the *effectively codable color volume* according to Eq. (27) by considering the impact of the discretization. Figure 2 shows the evaluation of a couple of well known *RGB* standards (with exclusion of *e-sRGB*) at variable bit rates. The figure presents the difference of the real-world surface color volume, which should be achieved by a good *RGB* encoding, relative to the actually attained one. While conventional color volume measures are not sensitive to bit resolution and thus stay at constant values while the bit rate is varied, the drop in the revised color volume with a decreasing number of bits becomes obvious. The results make evident that assigning less than 8 bits per *RGB* channel in general yields unacceptable deficits in the color encoding capability, since the color graduation gets too coarse. Encoding with 8 bits seems to be just the minimally required rate for an acceptable resolution. The evaluation is based on the discernible color limit of $\Delta E_{76}=1$.

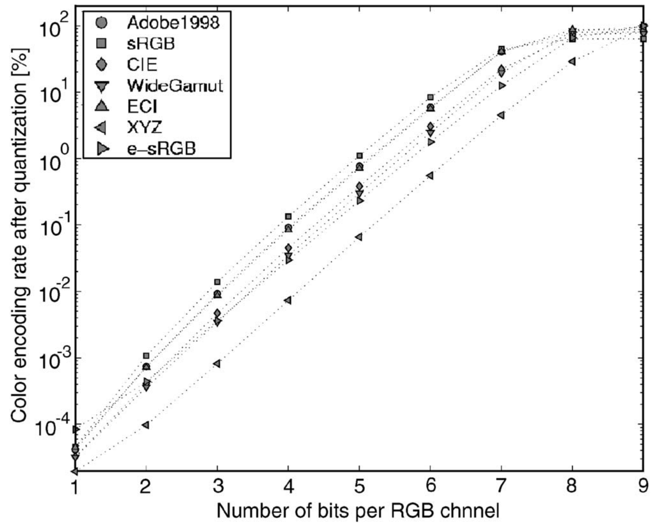

Figure 2. This figure illustrates the impact of the quantization according to Eq. (27). The limitation to 1 ΔE_{76} of the color space fraction recordable with a single code yields substantial color space shortcomings whenever the bit rate of the *RGB* channels is too low. The figure presents the effective color encoding rates depending on the number of coding bits. Several important *RGB* types were evaluated. Generally, even at a bit rate of 7 bits, only about one third of the real-world surface colors are encodable due to the excessively large color gaps between two adjacent codes. At a bit rate of 8 bits, the sampling rate is reasonably close to the perceptible color resolution.

Figure 3 displays the volumetric rankings for all *RGB* types listed above, combined with the conventional measure of the mean color distance for every two adjacent color codes. An optimal *RGB* encoding would provide both a high coverage of all real-world surface colors and a preferably high resolution of the color encodings. The second goal agrees with a low mean color distance between adjacent codes. The scope favorable for *RGB* data encoding is outlined as a shaded area. It incorporates four *RGB* specifications *Adobe 1998, NTSC 1953, ECI*, and *Kodak Open Interchange RGB*. Though two candidates ROMM and *Wide Gamut RGB* include large parts of the real-world surface colors, their mean color distance is rather large. RGB candidates such as the widely used *sRGB*, as well as *SMPTE, Kodak DC*, and *PAL*, are not optimal in respect of either rating.

XYZ has been designed with the constraint of including the whole gamut of optimal surface colors with *xy* values within the interval of [0, 1]. If *XYZ* is used as an 8 bit data *RGB*, conventional volumetric inspections expect it to include the entire gamut volume of all optimal surface colors. Yet when considering a resolution of 8 bits, the measure of Eq. (27) reveals that it intrinsically holds only about 30% of the real-world surface colors.

The extended *e-sRGB* provides substantially improved quality for both measures at 10 and even at only 9 bits per R,G,B channel. While the measure of Eq. (27) makes evident that it covers 100% of all real-world surface colors for both bit rates, the mean color distance of two adjacent color codes is in the same range as the mean distance for "small"

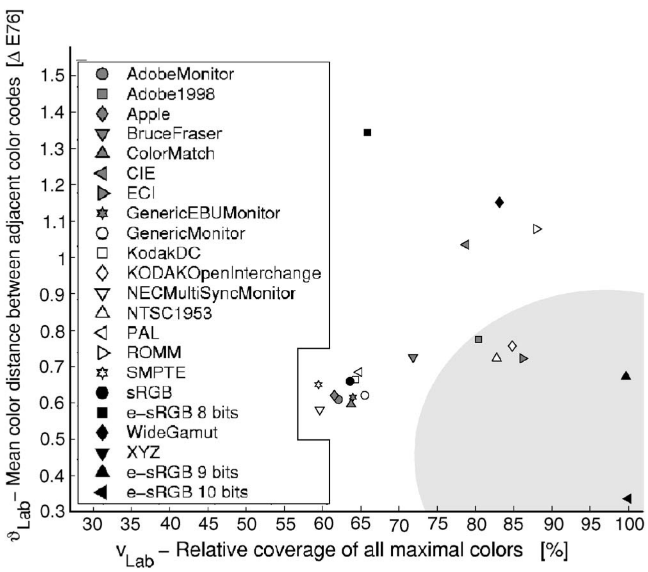

Figure 3. Evaluation of multiple *RGB* specifications according to the measures in Eqs. (27) and (28). The abscissa shows the effectively codable color volume in percent, that is, the percentage of all real-world surface colors being encodable with the respective *RGB* specifications. The ordinate points out the mean color difference between two adjacent color codes in ΔE_{76}. While the abscissa value ideally should approach 100%, the ordinate value is expected to be as small as possible. In addition to well-known conventional *RGBs*, the results obtained with the recently promoted *e-sRGB* are presented. In order to achieve an equitable comparison, the 8 bit analog version was analyzed, together with the considerably superior 9 and 10 bit versions. The preferable regions are emphasized with the shaded area. The particular values are listed in Table III.

conventional *RGB* types such as *sRGB*, and even far below in the case of 10 bits. That is, *e-sRGB* at 10 and even at 9 bits per channel, includes all practically existing surface colors at sufficient resolution.

In contrast, *e-sRGB* adapted to the familiar 8 bits *RGB* encoding provides insufficient benchmarks, especially with regard to the mean color distance between two color codes inside the gamut of the real-world surface colors.

Since getting along with one byte per channel is still a most interesting objective, the following sections focus on strategies for the amelioration of the *RGB* characteristics in terms of the measures discussed.

IMPROVED DATA *RGB* BASED ON THE *e-sRGB* CONCEPT

The *e-sRGB* standard provides outstanding advantages compared to *sRGB* or to other types of *RGB* specifications:

(1) The *e-sRGB* color set includes the complete space of all optimal surface colors, while according to the examinations presented in Sec. 3, *sRGB* for instance, includes only 35.8% of them. Moreover, *sRGB* provides only 63.8% even of the real-world surface color space, which is only half as large as the optimal surface color space. All values are based on the 3D considerations in Eq. (27).
(2) The resolution of *e-sRGB* is variable with 10, 12, or 16 bits per channel.
(3) The *e-sRGB* standard offers the same primary colors and the same gamma value as *sRGB*.

The drawbacks of *e-sRGB* are listed below:

(1) 70.72% of all *e-sRGB* color codes are located outside the optimal surface color gamut and hence are useful for recording self illuminants only. 50.76% of them exhibit negative X, Y, or Z tristimulus components, which are of very low significance. All values are referred to the 3D considerations in Eq. (27).
(2) If more than 10 bits per channel are used for *e-sRGB*, a 32 bit data word is not sufficient for including a full true color *RGB* color encoding. On the other hand at 10 bits per channel, the color codes within the optimal surface color gamut are far away from each other by up to 3.04 Δ_{E76} at high saturations, and within the real-world surface color gamut by up to 1.11 Δ_{E76}.
(3) The *e-sRGB* color codes may achieve negative *RGB* numbers which only exist in virtual color spaces. Yet, if an *RGB* is merely designed to be a data encoding system without any need for real-world scenarios, this is not a handicap.

Due to the benefits of *e-sRGB* which are achieved by an intelligent mapping of the *RGB* color values into the encoding space, the *e-sRGB* concept is well suitable for the basic concept when searching for an improved data *RGB*.

The degrees of freedom for such an *e-sRGB* analog are:

(1) The color values of the **R**, **G**, **B** primaries (6 degrees of freedom, see below);
(2) the gamma exponent γ of the power function (1 degree of freedom);
(3) as well as two parameters ε, ω for each R,G,B channel for the linear mapping into the encoding space ($3 \times 2 = 6$ degrees of freedom).

The *RGB* primary colors can be defined by its three-dimensional *XYZ* chromaticity values, or alternatively by its two-dimensional xy color table values plus the xy value of the white point (its luminance is supposed to be $Y=100$), forming 9 degrees of freedom, altogether. According to Sec. 3 by choosing the second option, a well defined white point guarantees a color neutral gray axis, while 6 degrees of freedom remain for the *RGB* primaries.

Hence for the *e-sRGB* concept, a total of 13 degrees of freedom is available for optimization.

An optimized *RGB* is determined according to the following rules:

(1) The *e-sRGB* concept is adopted and optimized accordingly.
(2) By selecting suitable parameters for mapping the *RGB* values onto the coding space, the faces of the *RGB* cube are shifted such that they closely snuggle around the real-world surface color gamut. This

alignment satisfies the variables for the linear mapping, i.e., 6 degrees of freedom. The current *e-sRGB* standard wastes a lot of encoding space for colors beyond the real-world and even the optimal surface color gamut.

(3) The xy values for the primaries definition and the gamma value make up a seven-dimensional space which is available for further optimization. The measures developed in Sec. 3 are chosen as target functions.

Revised Linear Mapping of the RGB *Values into Encoding Space*

The linear mapping of the *RGB* values into the n-bits coding range provides two free parameters ε and ω for each channel. According to Sec. 3, an optimal data *RGB* should be able to encode all real-world surface colors inside of the gamut of the real-world surface colors, while colors outside the optimal surface color gamut are a waste of bit resources. Thus, a new approach is suggested by assessing ε and ω such that the *RGB* faces at $C''=0$ and $C''=2^n-1$ (notation see Sec. 2) are tangents to the surface of the real-world surface color space $\mathcal{O}$.

Considering a data range codable with n bits such that

$$C'' \in [0,1,\ldots,2^n-1], \tag{31}$$

the linear mapping with Eq. (4) deforms the encodable data range to

$$C' \in \left[\left(-\frac{\omega}{\varepsilon}\right),\ldots,\left(-\frac{\omega}{\varepsilon}+\frac{i}{\varepsilon}\right),\ldots,\left(-\frac{\omega}{\varepsilon}+\frac{2^n-1}{\varepsilon}\right)\right],$$

$$i \in \{1,2,3,\ldots\}. \tag{32}$$

If the set of all optimal surface colors $RGB' \in \mathcal{O}$ is considered, let its boundary RGB' values be denominated by $C'_{\min}$ and $C'_{\max}$ with $C' \in \{R',G',B'\}$. With

$$C' \in [C'_{\min},\ldots,C'_{\max}], \tag{33}$$

and Eq. (32) can be deduced

$$\varepsilon = \frac{2^n-1}{C'_{\max}-C'_{\min}}, \tag{34}$$

$$\omega = -C'_{\min}\cdot\frac{2^n-1}{C'_{\max}-C'_{\min}}. \tag{35}$$

The resulting ε_R, ε_G, ε_B and ω_R, ω_G, ω_B values are channel specific and define the required linear mapping parameters where the faces of the *RGB* cube are shifted as close as possible towards the optimal surface color space boundaries.

RGB Primaries and Gamma Value Optimization

The remaining free parameters, the xy chromaticity values of the primaries x_R,y_R,x_G,y_G,x_B,y_B, as well as the gamma value γ — 7 degrees of freedom altogether — are optimized according to the metrics proposed in Sec. 3.

No constraints are assumed to be accounted for the optimization process of this seven-dimensional vector space. The omission of constraints in principle causes the primaries and the gamma value to achieve arbitrary values. Hence, optimization might eventually bring forth primary values beyond the scope of human perception. This is unfavorable whenever the *RGB* definition is intended to represent an existing image reproducing device. Yet, the exclusive data *RGB* on which this paper is focused is expected to require some matrix transformation in order to be suitable for real color applications.

Without imposing constraints, the multidimensional Nelder-Mead simplex search method for iterative unconstrained minimization[30,31] is well suited as the principal optimization algorithm.

Provided that the data mapping onto the coding space is accomplished according to Sec. 4.1, the resulting *RGB* volume will include at least the complete gamut of real-world surface colors. Consequently, any shortcomings still remaining in the color coverage are caused by insufficient bit resolution and/or a perceptibly inhomogeneous code distribution.

RESULTS: RATING OF THE REFINED RGB ENCODING

The *RGB* set in Table II has been redesigned according to the propositions of Sec. 4.1 by redesigning the linear mapping of the *RGB* colorimetry values into the encoding space. Thereby, the encoding coefficients ε and ω have been optimized for each *RGB* channel separately according to Eqs. (34) and (35). The resulting *RGB* encodings have subsequently been validated with the estimation criteria ν_{Lab} and ϑ_{Lab} [Eqs. (28) and (27)] as proposed in Sec. 3.

Figure 4 shows the evaluations of basically the same *RGB* encodings as of those in Fig. 3. The figure gives the validation of each original encoding scheme together with its refined version. The ratings are displayed as tuples of two values connected by a line, each, starting with the ratings of the original *RGB* definition emphasized with small symbols, and ending with the ratings of the enhanced encoding marked with large symbols. The results indicate a remarkable improvement of criteria ν_{Lab} after the refinement. This holds true for all considered *RGB* definitions. Regardless of the validations of the ordinary *RGB* encodings, which often show an effective coverage of less than 65% of the real-world surface color space only, most of the assessments taken *after* the modification achieve values of more than 90%.

On the other hand it has to be stated that a large amount of the refined *RGB* schemes attain at slightly increased mean color difference values ϑ_{Lab} [Eq. (28)]. Fortunately, the augmentation of ϑ_{Lab} is quite moderate and hardly exceeds values of more than 10%. Moreover, the ϑ_{Lab} values remain below the critical limit of 1 ΔE in most of all cases, except for those where already the original ϑ_{Lab} exceeds 1 ΔE, where ϑ_{Lab} even decreases after the *RGB* refinement.

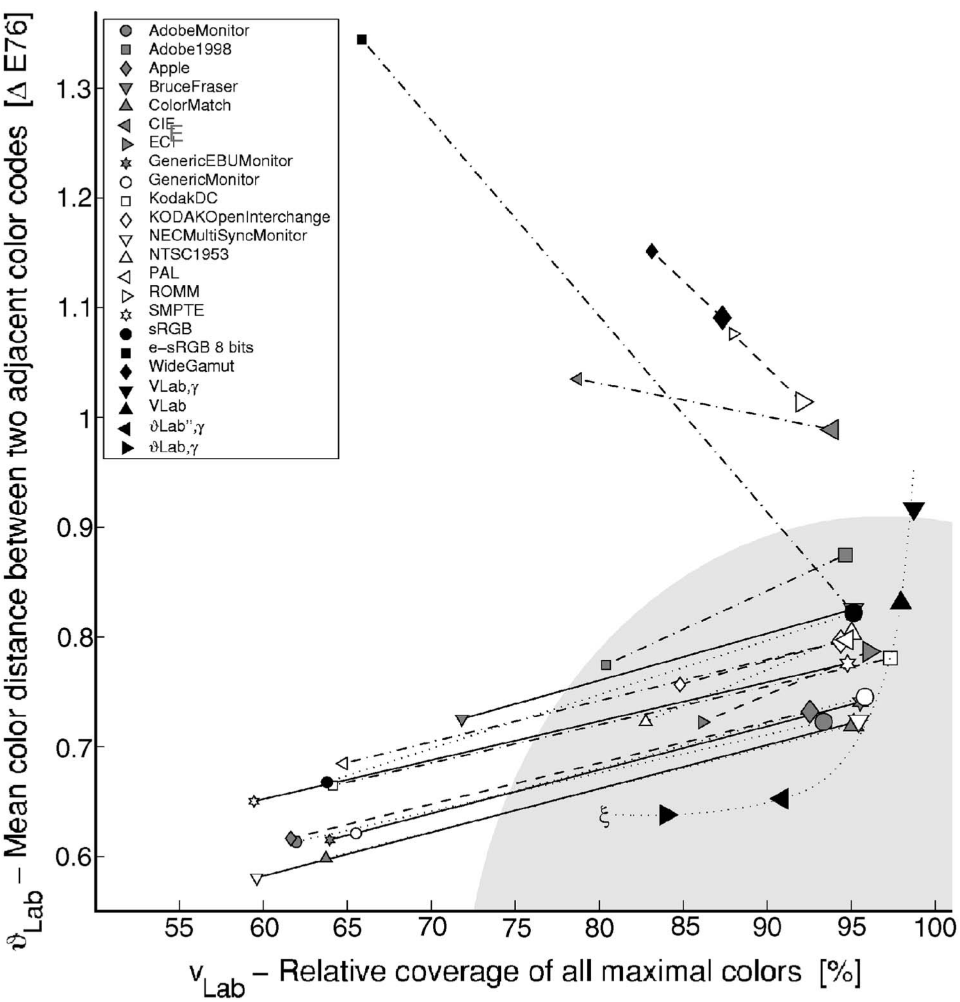

Figure 4. Improvement of the *RGB* specifications of Table II when applying the e-sRGB concept optimized according to Sec. 4.1 and evaluating with the same measures as in Fig. 3. The enhancement is illustrated by straight lines starting from the ratings of the unchanged original *RGB* (small symbol) and ending with the estimations of the respective extended and revised *RGB* (8 bits), using the equivalent primary colors and gamma values (large symbols). The results prove a considerable upgrade of all *RGB* types with respect to the effectively codable color volume according to Eq. (27), showing increased real-world surface color codability rates over 95%. Yet, most of the mean color distances increase somewhat, although they are usually still clearly below 1 ΔE. In addition, this figure shows the values of some optimized *RGB*. The focused optimization criteria are minimal v_{Lab}, ϑ''_{Lab}, and ϑ_{Lab} (see measures 27, 29, and 28 of to Sec. 3.3). The optimizations were performed by varying the primaries, and by taking either fixed or variable gamma values γ. The particular values are listed in Tables III and IV.

Beside the enhanced results obtained from the measure v_{Lab} it is important to keep in mind that in case of the traditional *RGB* encoding, the codable color space is restricted to the triangle spanned by the primary colors, while the enhanced *e-sRGB* concept in contrast allows the description of colors within the full real-world surface color gamut (Sec. 3.1), which is an outstanding improvement.

The progression of the *sRGB* and of the *e-sRGB* encoding might be especially pointed out. The well established *sRGB* whose assessment is displayed with a black circle exhibits a fairly low rating in terms of v_{Lab} due to its comparatively small color volume, as already stated in Sec. 3. The same holds true for *e-sRGB* (marked with a black square) for a resolution of 8 bits per channel. In the case of the 8 bit *e-sRGB*, the low assessment value arises solely from the coarse discretization, while from a purely geometrical point of view, the color space spanned by *e-sRGB* is even *larger* by far than the gamut of the optimal surface colors boundaries (Sec. 3.1). Besides the low v_{Lab} rating, the mean color distance ϑ_{Lab} between two adjacent codes is $\Delta E = 1.34$ and thus larger than approved. As a matter of course, both *sRGB* and *e-sRGB* end up in the same refined encoding. It features an excellent value of $v_{Lab} = 95.1\%$ and a reasonably low $\vartheta_{Lab} = 0.82 \Delta E$.

The ratings of the enhanced *RGB* settings listed in Table II clearly exhibit considerable variation depending on the primaries' locations and the gamma values. This fact begs the question as to the best *RGB* settings yielding a real-world surface color volume coverage v_{Lab}, a minimal mean color distance value ϑ_{Lab}, or ideally, both. An appropriate optimization strategy based on the Nelder-Mead simplex search algorithm has been used according to Sec. 4.2. Variable tar-

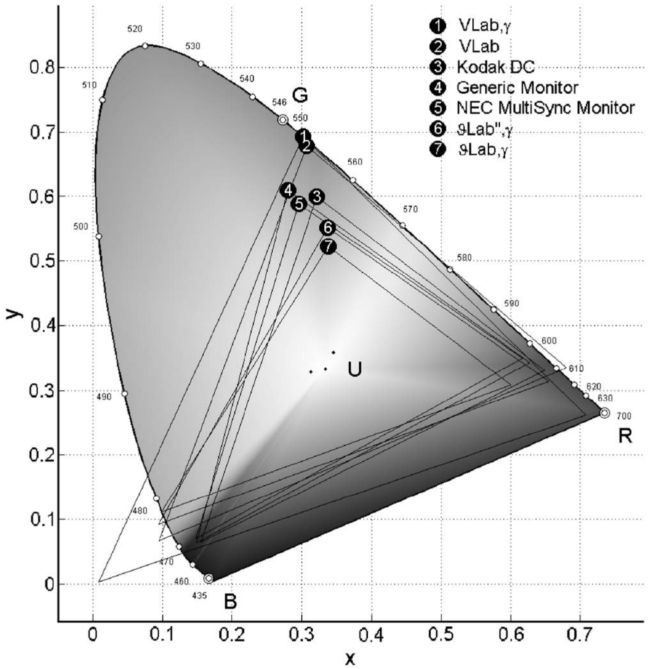

Figure 5. *RGB* primaries optimized towards minimal v_{Lab}, ϑ''_{Lab} and ϑ_{Lab} (see measures 27, 29, and 28 of to Sec. 3.3). The optimized degrees of freedom are the primary locations x_R, y_R, x_G, y_G, x_B, y_B, and the gamma value γ. In the case of v_{Lab}, one of the two optimizations was performed with a fixed gamma of γ=2.4. The figure shows the well-known horseshoe shaped xy color space representation. The particular *RGB* specification values are given in Table V. Please notice that the triangular shapes are plotted for the purpose of clarity only, and do not indicate color boundaries as in conventional *RGB*.

get measures have been chosen for minimization, including $V_{\mathrm{ref}}-V_{Lab}$, ϑ_{Lab}, ϑ''_{Lab}, and ψ_{Lab} (measures 27, 28, 29, and 30). Alternatively, only the x,y-chromaticities of the *RGB* primaries supplying 6 degrees of freedom (Sec. 3.2) have been chosen as free parameters, or the primaries x,y-chromaticities together with the gamma value, yielding a total of 7 free parameters.

The iterative optimizations usually converged after 200–800 iterations. Some of the results are included in Fig. 4. The highest value for the effectively color volume was found at v_{Lab}=98.7% (see identifier "$V\,Lab,\gamma$") by minimizing $V_{\mathrm{ref}}-V_{Lab}$, The maximization of V_{Lab} was, however, inevitably associated with an elevated ϑ_{Lab}=0.917 value. On the other hand, the lowest value found for ϑ_{Lab}=0.638 comes along with a lower percentual color coverage value of v_{Lab}=84.0% (see identifier "$\vartheta Lab,\gamma$").

The two estimates above are part of the envelope ξ which includes the locations of all optimal *RGB* settings featuring the feasible limit for the measures v_{Lab} and ϑ_{Lab} at 8 bits per *RGB* channel. Since thousands of refined *RGB* calculations have been performed during the optimization processes, the envelope ξ could well be determined numerically. It is plotted as a dotted line in the lower right half of Fig. 4.

Beside the extreme findings at "$V\,Lab,\gamma$" and "$\vartheta\,Lab,\gamma$," the envelope ξ includes some further exclusively selected points which are displayed in Fig. 4. The one identified with "$\vartheta Lab'',\gamma$" represents the value attained when optimizing for the minimal mean square root ϑ''_{Lab}, while the one identified with "$V\,Lab$" stands for the minimization of $V_{\mathrm{ref}}-V_{Lab}$. In the latter case, the gamma value has been fixed to γ=2.4 according to some commonly known *RGB* types (e.g., *sRGB* and *e-sRGB*).

Table III. Ratings of the original (ori.) and the refined (ref.) versions of some selected *RGB* types. The refined versions have been enhanced according to the concept proposed in Sec. 4. Detailed encoding specifications are given in Tables I and V.

RGB Type		v_{Lab} [%]	ϑ_{Lab}	ϑ''_{Lab}	ψ_{Lab76}	ψ_{Lab94}
sRGB	ori.	63.8	0.668	0.675	1.176	0.931
e-sRGB	ori.	65.9	1.344	1.363	4.443	1.850
e-sRGB	ref.	95.1	0.822	0.833	3.801	1.093
Adobe1998	ori.	80.4	0.775	0.789	1.614	1.240
	ref.	94.7	0.875	0.891	2.543	1.376
Color Match	ori.	63.7	0.598	0.611	1.654	1.309
	ref.	95.1	0.720	0.747	4.066	1.470
ECI	ori.	86.1	0.722	0.737	1.986	1.560
	ref.	96.1	0.787	0.804	2.565	1.667
Generic Monitor	ori.	65.5	0.621	0.634	1.583	1.239
	ref.	95.8	0.745	0.770	3.692	1.404
KodakDC	ori.	64.2	0.665	0.673	1.286	1.021
	ref.	97.3	0.781	0.795	4.071	1.130
NEC Multi Sync	ori.	59.6	0.581	0.592	1.491	1.158
	ref.	95.4	0.723	0.751	4.081	1.346
ROMM	ori.	88.0	1.076	1.086	1.993	1.613
	ref.	92.1	1.014	1.024	1.868	1.529
Wide Gamut	ori.	83.1	1.151	1.169	2.086	1.701
	ref.	87.3	1.091	1.107	1.961	1.610

Table IV. Ratings of some new optimized *RGB* specifications (see Sec. 5), enhanced according to the concept proposed in Sec. 4. Detailed encoding specifications are given in Tables I and VI.

Optimization Criteria	v_{Lab} [%]	ϑ_{Lab}	ϑ''_{Lab}	ψ_{Lab76}	ψ_{Lab94}
$V\,Lab,\ \gamma$	98.7	0.917	0.918	2.134	0.967
$V\,Lab$	98.0	0.831	0.839	2.964	1.134
$\vartheta Lab'',\ \gamma$	90.9	0.653	0.690	4.941	1.624
$\vartheta Lab,\ \gamma$	84.0	0.638	0.714	5.810	2.042

Table V. Encoding specifications of some well-known *RGB* types which are enhanced according to the refined *e-sRGB* concept of Sec. 4. The table includes the mapping parameters ε and ω (optimized), the chromaticity values of the primaries, the gamma value, as well as the white point (original specifications). The associated ratings are given in Table III.

	ε_R ε_G ε_B	ω_R ω_G ω_B	x_R x_G x_B	y_R y_G y_B	γ	W
	127.500	96.000	0.6400	0.3300		
e-sRGB (*original*)	127.500	96.000	0.3000	0.6000	2.40	D65
	127.500	96.000	0.1500	0.0600		
	152.131	71.778	0.6400	0.3300		
e-sRGB (*refined*)	217.057	42.148	0.3000	0.6000	2.40	D65
	198.358	61.865	0.1500	0.0600		
	190.047	48.194	0.6400	0.3300		
Adobe1998	220.966	38.636	0.2100	0.7100	2.20	D65
	213.950	47.446	0.1500	0.0600		
	170.653	50.704	0.6300	0.3400		
Color Match	222.680	37.759	0.2950	0.6050	1.80	D50
	204.746	56.822	0.1500	0.0750		
	211.346	29.119	0.6700	0.3300		
ECI	233.582	26.994	0.2100	0.7100	1.80	D50
	232.712	30.701	0.1400	0.0800		
	176.274	49.493	0.6277	0.3427		
Generic Monitor	219.189	41.011	0.2803	0.6097	1.90	D50
	199.686	61.312	0.1491	0.0636		
	152.902	68.633	0.6492	0.3314		
KodakDC	220.551	39.010	0.3219	0.5997	2.22	D50
	203.576	57.178	0.1548	0.0646		
	167.653	54.672	0.6167	0.3503		
NEC Multi Sync	213.967	46.070	0.2957	0.5884	1.90	D50
	195.929	64.771	0.1481	0.0697		
	257.564	2.947	0.7347	0.2653		
ROMM	260.014	0.435	0.1596	0.8404	2.20	D50
	263.832	0.000	0.0366	0.0001		
	217.681	32.062	0.7347	0.2653		
Wide Gamut	260.631	0.000	0.1152	0.8264	2.20	D50
	237.595	24.868	0.1566	0.0177		

While the above mentioned values for ξ refer to *RGB* characteristics achieved by explicit optimization, the envelope ξ also passes close by ratings referring to enhanced versions of some well-known *RGB* characteristics. This *RGB* category includes in particular "Kodak DC," "Generic Monitor," and "NEC Multi Sync Monitor" *RGB*.

Some of the above mentioned optimal *RGB* specifications are displayed in Fig. 5 in the chromaticity diagram. The figure shows that the optimal *RGB* triangles do not fundamentally differ from typical *RGB* characteristics like those of Fig. 1. Though most of the primaries remain inside the spectrum locus, some of them do not. This is however alright if an *RGB* is exclusively designed for encoding purpose.

A list of the assessment values for a few selected ratings is given in Tables III and IV. The set in Table III includes the values $\nu_{Lab}[\%]$, ϑ_{Lab}, ϑ''_{Lab}, ψ_{Lab76}, and ψ_{Lab94} [Eqs. (27)–(30)] of some original *RGB* characteristics, as well as of their refined versions. In Table IV, the ratings are provided for the optimized *RGB* specifications discussed above. While in general, the original color coverage is only on the order of about 70%, the refined *RGB* types achieve ν_{Lab} values of around 95%. The mean color distance ϑ_{Lab} between two adjacent color codes usually slightly increases after the refinement; however, it remains below 1 in the majority of cases. The same holds true for the quadratic mean color distance ϑ''_{Lab}.

Finally, the maximal color distance between two adjacent color codes ψ_{Lab} was examined. It appears that this value exceeds the 1 ΔE limit by a factor of more than 2 up to almost 6 for all of the refined *RGB* versions. The conventional *RGB* estimations in contrast exhibit acceptable maximal distances of a ΔE between 1 and 2. The suspicion was obvious that the high maximal distances at refined *RGB* versions are supposedly achieved at high saturations where the ΔE_{76} based measures associated with the *Lab* rating are known to produce excessive values. Since the conventional *RGB* encodings generally enclose lower saturations than the refined ones, they would consequently yield lower maximal color distances.

This speculation was confirmed by recomputing the distance values using the ΔE_{94} measure. The resulting values are given with ψ_{Lab94} in the right column of Tables III and IV. Evidently, the ΔE_{94} measure exhibits a significantly lower discrepancy between the maximal color distances of conventional and refined *RGB* types, compared to the ΔE_{76} measure. For both *RGB* types, the values are now in the same range between 1 and 2.

Table V lists the specifications of the refined *RGB* types considered, including the encoding parameters ε and ω for each *RGB* channel, as well as the respective chromaticity values of the primaries, the gamma values, and the white points, which are original. Table VI lists the respective specifications for the new optimized *RGB* settings discussed above. Notice that some of the primaries are outside the spectrum locus. However, this is irrelevant as long as the *RGB* is used exclusively for the purpose of data storage.

Table VI. Encoding specifications of some new optimized *RGB* specifications, enhanced according to the refined *e-sRGB* concept of Sec. 4. The table includes the mapping parameters ε and ω, the chromaticity values of the primaries, the gamma value, as well as the white point (all specifications optimized). The associated ratings are given in Table IV.

	ε_R ε_G ε_B	ω_R ω_G ω_B	x_R x_G x_B	y_R y_G y_B	γ	W
	203.729	50.273	0.708 026	0.261 757		
V Lab, γ	254.651	4.597	0.302 160	0.693 429	2.865 456	D65
	234.258	26.913	0.008 690	0.002 970		
	185.886	54.265	0.679 895	0.334 856		
V Lab	213.508	45.321	0.306 477	0.678 825	2.40	D65
	263.091	0.000	0.094 873	0.066 509		
	158.067	61.641	0.655 421	0.313 606		
, γ	220.857	34.030	0.336 601	0.551 851	1.611 455	D65
	210.637	51.819	0.094 276	0.092 726		
	150.673	61.492	0.599 914	0.308 644		
ϑ_{Lab}, γ	209.796	36.822	0.337 655	0.522 399	1.422 382	D65
	197.246	64.460	0.098 509	0.111 208		

CONCLUSIONS

The topic of profitable *RGB* setting was analyzed with the exclusive focus on optimal data encoding. The current *RGB* situation was discussed and a valuation strategy proposed for the judgment of *RGB* specifications. The measures suggested give an estimate for the fraction of the actually existing surface colors being encodable with a certain *RGB*. The metrics combine the codable color gamut volume with discretization related attributes.

Various well-known *RGB* definitions were examined according to this evaluation scheme. It turns out that all of them suffer from considerable deficits in the encodable color volume when accounting for real-world surface colors.

The recently promoted *e-sRGB* concept was shown to be an outstanding *RGB* alternative. Attempts to validate it in its present state does not exhibit many benefits when examining it at a resolution of 8 bits per *RGB* channel (which is not provided for the *e-sRGB* standard). However, a suitable refinement strategy of the *e-sRGB* concept providing a substantial upgrade in respect of the above rating was proposed in this paper.

Various *RGB* configurations were modified applying the refined *e-sRGB* concept. The rating results clearly reveal its excellent ranking compared to all conventional *RGB* types.

Additionally, an attempt is suggested for optimizing the primaries and the gamma value. The optimization results reveal the limitations of the proposed *RGB* concept and identify the *RGB* settings for *Kodak DC, Generic Monitor, and NEC Multi Sync Monitor* to be especially advantageous if the refined *e-sRGB* concept is applied to them.

In summary, the new refined *e-sRGB* strategy features an outstanding improvement in respect of the codable color volume when compared with conventional *RGB* encodings. The new strategy permits the composition of essentially enhanced *RGB* definitions using the traditional 3×8 bit arrangement.

ACKNOWLEDGMENTS

This work has been partly supported by cooperation from the International Newspaper Color Association (*ifra*) in Darmstadt, Germany, the Swiss Federal Laboratories for Materials Testing and Research (*EMPA*) St. Gallen, Switzerland, and the Association for the Promotion of Research in the Graphic Arts Industry (*Ugra*). All contributions are gratefully annotated.

REFERENCES

[1] G. Wyszecki and W. Stiles, *Color Science* (Wiley-Interscience, New York, 1982).

[2] IEC 61966–2.1. Multimedia systems and equipment—Color measurement and management—part 2-1: Color management—Default RGB color space—*sRGB*. Technical report, 1999.

[3] IEC/ISO FDIS 61966-2-1 A1. Amendment 1 to Multimedia systems and equipment—Color measurement and management—part 2-1: Color management—Default RGB color space—*sRGB*. Technical report, 1999.

[4] M. Anderson, R. Motta, S. Chandrasekar, and M. Stokes, "Proposal for a standard default color space for the internet: *sRGB*", *Proc IS&T/SID's Fourth Color Imaging Conference* (IS&T, Springfield, VA, 1995) pp. 238–245.

[5] Graphic technology—Process control for the manufacture of half-tone color separations, proofs and production prints—Part 3: Coldset offset lithography and letterpress on newsprint, Technical report, ISO 12647-3 1998.

[6] S. Susstrunk, R. Buckley, and S. Swen, "Standard *RGB* color spaces", *Proc. IS&T/SID's 7th Color Imaging Conference* (IS&T, Springfield, VA, 1999) pp. 127–134.

[7] K. E. Spaulding and J. Holm, "Color encodings for digital photofinishing", *Proc. IS&T's 12th International Symposium on Photofinishing Technologies* (IS&T, Springfield, VA, 2002) pp. 91–96.

[8] K. E. Spaulding, G. J. Woolfe, and E. J. Giorgianni, "Optimized extended gamut color encoding for scene-referred and output-referred image states", J. Imaging Sci. Technol. **45**(5), 418–426 (2001).

[9] K. E. Spaulding, G. J. Woolfe, and E. J. Giorgianni, "Image states and standard color encodings (RIMM/ROMM RGB)", *Proc. IS&T/SID's 8th Color Imaging Conference* (IS&T, Springfield, VA, 2000) pp. 288–294.

[10] G. W. Larson, "Overcoming gamut and dynamic range limitations in digital images," *Proc. IS&T/SID's Sixth Color Imaging Conference* (IS&T, Springfield, VA, 1998) pp. 214–219.

[11] Photography—Electronic Still Picture Imaging—Extended *sRGB* Color Encoding—*e-sRGB*. Technical report, Photographic and Imaging Manufacturers Association, Inc. (PMA, Harrison, NY, 1996).

[12] M. Stokes, M. Anderson, S. Chandrasekar, and R. Motta. A Standard Default Color Space for the Internet—*sRGB*, http://www.w3.org/Graphics/Color/sRGB; http://apphost.infosrc.com/icc/sRGB.html (November 1996).

[13] Photography and graphic technology—Extended color encodings for digital image storage, manipulation and interchange—Part 1: Architecture and requirements. Technical report, ISO 22028-1, 2004.

[14] G. D. Finlayson and S. Susstrunk, "Optimization for hue constant RGB sensors", *Proc. IS&T/SID's 10th Color Imaging Conference* (IS&T, Springfield, VA, 2002) pp. 343–348.

[15] E. M. Granger, "A vision based RGB color space", *Proc. TAGA*, 318–332 (2001).

[16] H. R. Kang, "Computational accuracy of RGB encoding standards", *Proc. IS&T's NIP19* (IS&T, Springfield, VA, 2000) pp. 661–664.

[17] J. Katajamäki and P. Laihanen, "Image dependent gamma selection based on color palette equalization and a simple lightness model", *Proc. IS&T/SID's 7th Color Imaging Conference* (IS&T, Springfield, VA, 1999) pp. 301–306.

[18] B. Hill, Th. Roger, and F. W. Vorhagen, "Comparative analysis of the quantization of color spaces on the basis of the CIELAB color-difference formula", ACM Trans. Graphics **16**(2), 109–154 (1997).
[19] K. Spaulding and G. Braun, "Method for evaluating the color gamut and quantization characteristics of output-referred extended-gamut color encodings", *Proc. IS&T/SID's 10th Color Imaging Conference* (IS&T, Springfield, VA, 2002) pp. 99–105.
[20] G. T. Fechner, *Elemente der Psychophysik* (Breitkopf und Härtel, Leipzig, 1860).
[21] E. Schördinger, "Theorie der pigmente von grösster leuchtkraft", Ann. Phys. (Paris) **4**(62), 603–622 (1920).
[22] M. R. Pointer, "The gamut of real surface colors", Color Res. Appl. **5**(3), 145–155 (1980).
[23] U. Steingrímsson, K. Simon, W. Steiger, and K. Schläpfer, "The gamut obtainable with surface colors", *Proc. IS&T/SID's First CGIV Conference* (IS&T, Springfield, VA, 2002) pp. 287–291.
[24] J. Tajima, H. Haneishi, N. Ojima, and M. Tsukada, "Representative data selection for standard object color spectra database (SOCS)", *Proc. IS&T/SID's 10th Color Imaging Conference* (IS&T, Springfield, VA, 2002) pp. 155–160.
[25] K. M. Lam, "Metamerism and color constancy", Ph.D. thesis, 1985, University of Bradford, Bradford, UK.
[26] A. R. Robertson, "The CIE 1976 color-difference formulae", Color Res. Appl. **2**(1), 7–11 (1977).
[27] J. O'Rourke, *Computational Geometry in C*, 2nd ed. (Cambridge University Press, Cambridge, 1999).
[28] National Science, Technology Research Center for Computation, and Visualization of Geometric Structures (The Geometry Center, University of Minnesota, http://www.geom.uiuc.edu/ 1993).
[29] R. W. G. Hunt, *The Reproduction of Color in Photography, Printing and Television* (Fountain Press, Tolworth, UK, 1987).
[30] R. Chelouah and P. Siarry, "Genetic and Nelder-Mead algorithms hybridized for a more accurate global optimization of continuous multiminima functions", Eur. J. Oper. Res. **148**(2), 335–348 (2003).
[31] M. A. Luersen and R. Le Riche, "Globalized Nelder-Mead method for engineering optimization", *Proc. Third International Conference on Engineering Computational Technology* (Civil-Comp Press, Stirling, UK, 2002) pp. 165–166.
[32] US Standard ANSI/I3A IT10.7666. Photography—Electronic Still Picture Imaging—Reference Output Medium Metric RGB Color Encoding (ROMM RGB). Technical report, 2003.